View metadata, citation and similar papers at core.ac.uk
brought to you by CORE
provided by The Australian National University

N+ REGIONS FORMED BY PHOSPHORUS IMPLANTATION AND SOLID PHASE EPITAXIAL REGROWTH

T. J. Ratcliff, K. C. Fong, A. W. Blakers
Centre for Sustainable Energy Systems, Australian National University
Building 32, North Road, 0200, Canberra, Australia
Ph: +612 6125 0078, Fax: +612 6125 8873, Email: tom.ratcliff@anu.edu.au

ABSTRACT: Damage to the target wafer is an unavoidable characteristic of ion implantation. Provided sufficient damage is created in the target wafer, an amorphous region will form which may then be recrystallised by solid phase epitaxial regrowth. In this study, phosphorus ions were implanted at varied dose and energy into crystalline silicon wafers and annealed at 600°C for 10 minutes to allow for epitaxial regrowth. It is found that this annealing regime activates dopants within the regrown amorphous layer, however the J_{0n+} after SPER is significantly higher compared with equivalent samples that were annealed at high temperature. We attributed this to increased S-R-H recombination in regions damaged, but not amorphised, during implantation. Due to high active dopant concentration after recrystallisation, phosphorus implantation and SPER may present a low thermal budget alternative for forming localised N+ regions under electrical contacts.
Keywords: annealing, contact, epitaxy, n-type

1 INTRODUCTION

Ion implantation is an alternative to thermal diffusion for forming heavily doped regions in a solar cell. It is a single-sided and easily masked process offering excellent control and repeatability. These advantages have been leveraged in both high efficiency laboratory devices [1] and industrial manufacturing processes [2]. However, ion implantation invariably damages the target substrate.

Damage is created when implanted dopant atoms collide with atoms in the crystal of the target wafer, displacing atoms of the target wafer, resulting in vacancy and interstitial defects populating the crystal lattice. In addition, implanted dopant atoms come to rest in interstitial locations, where they are not electrically active. Should a sufficient number of silicon atoms be displaced, the local crystalline structure of the target wafer is destroyed and a continuous amorphous layer is formed at the surface of wafer [3]. Regions that are not sufficiently damaged will not be amorphised but instead retain a 'damaged crystalline' structure. The amount of damage created during implantation depends on a range of factors, including implant dose, energy, dose rate, the mass of the implanted species and wafer temperature during implantation.

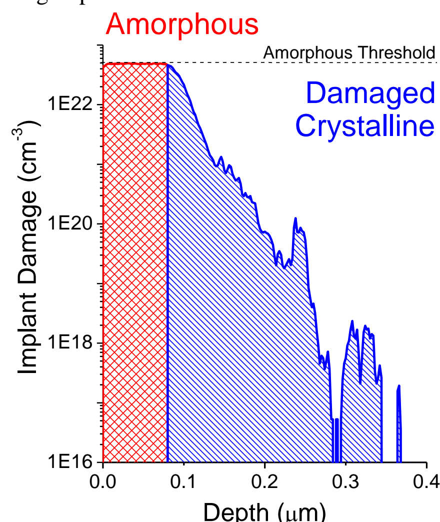

Figure 1: Primary implant damage for 3E15 cm^{-2} P implant at 40 keV as simulated in Sentaurus Process.

A simulated damage profile resulting from a 3×10^{15} cm^{-2} at 40 keV is displayed in Figure 1. This image shows the characteristics of an amorphising implant, with an amorphous region at the surface shown in red and the damaged crystalline region at the tail of the implant is represented by the blue area. The upper limit for damage concentration is the amorphous threshold, 5×10^{22} cm^{-3} in this simulation [4]. The transition from a damaged crystalline structure to a completely amorphous layer requires the concentration of implant damage to exceed this threshold. Any damage beyond the amorphous threshold does not further damage the target material.

In order to completely repair implant damage and activate all implanted dopant atoms, a long, high temperature furnace anneal is required. However, the dopant atoms contained within the amorphised layer may be activated at low temperature using solid phase epitaxial regrowth.

Solid phase epitaxial regrowth, SPER, is the directional recrystallisation of an amorphous material in direct contact with a crystalline material. Atoms within the amorphous solid rearrange to join the structure of the adjacent crystalline region, extending the crystalline structure at the amorphous/crystalline interface, layer by layer [5]. The advancing interface activates dopant atoms and repairs implant damage in the amorphised region.

SPER is initiated when a wafer with an amorphous region on a crystalline substrate is exposed to sufficient temperature. The crystalline interface advances into the amorphous region at a rate that is strongly dependent on temperature. For example, complete recrystallisation of a 100nm amorphous layer will take more than one hour at 500°C, but less than 1 minute at 600°C and less than 3 seconds at 700°C [5].

When the annealing regime is limited to allow SPER, very little thermal diffusion would be expected to occur. The result is an active dopant profile after SPER that closely resembles the as-implanted profile, retaining the high concentration near the surface and shallow overall doping. The ability to tailor steep dopant profiles guarantees low contact resistance even with low implant dose.

Although SPER repairs and activates dopants in the amorphised region, the 'damaged crystalline' regions are not repaired. Instead, these regions require high temperature annealing, typically in excess of 900°C, to

activate dopants, repair primary implant damage and dissolve secondary defects, such as dislocation loops, that may form during the anneal [6].

In this study, the use of SPER is investigated as a low thermal budget technique for forming localised N+ regions directly under the contacts. Provided good electrical contact can be made, the localised N+ contact doping may be restricted to occupy only a fraction of total cell area, thus minimising the global impact of the highly recombining regions [7]. Furthermore, the low temperature requirements for SPER increase process flexibility and present the opportunity to complete the implant and activation steps after temperature sensitive steps. For example, implants may be performed through openings in a deposited dielectric layer. Subsequent high temperature processing may then be limited to preserve passivation or optical properties of the dielectric film. In such a process, the same openings in the dielectric may also be used during metallization to align the localised doping and contacts.

This is in contrast to a process where a thermal oxide may be grown during a high temperature anneal. While the higher temperature anneal would be expected to more thoroughly anneal the implant damage, further alignment is necessary to form the localised contact structure.

2 EXPERIMENTAL DETAILS

Chemically polished, 100Ω.cm FZ silicon wafers were implanted on both sides with $^{31}P^{-}$ at implant dose ranging from 1×10^{15} cm^{-2} to 3×10^{15} cm^{-2} and energies from 20keV to 160keV. All samples were implanted at a tilt of 7° relative to the implant beam to minimise the effects of implant channeling. Annealing steps were performed in a quartz oxidation furnace at 600°C for ten minutes in N_2. J_{0n+} was measured for entirely unpassivated samples in order to approximate the surface recombination velocity of a metallised surface. Contact resistance was measured using the TLM method, where photolithography was used to define contact pads of evaporated aluminium. Sintering of contacts was performed at 250°C for 30 minutes in a forming gas ambient.

3 RESULTS

3.1 Dopant Activation

The effectiveness of SPER to activate implanted dopant atoms was evaluated by measuring sheet resistance after anneal. Figure 2 shows that the sheet resistance decreases for increasing implant dose. This demonstrates that the implants are at least partially activated by the 600°C, ten minute anneal for all implant energy and dose investigated.

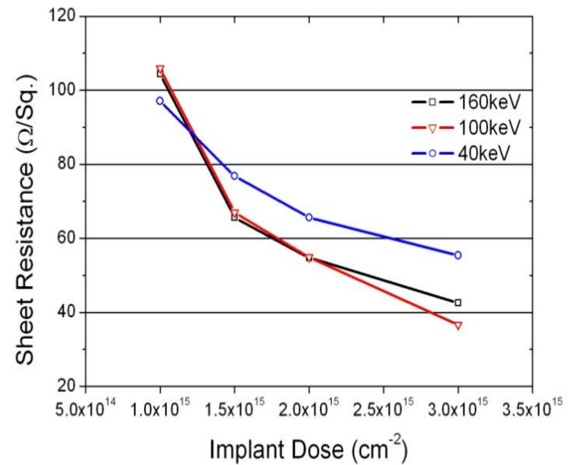

Figure 2: Sheet Resistance after solid phase epitaxial regrowth at 600°C for 10 minutes.

The active dopant profile for a 3×10^{15} cm^{-3} implant at 40 keV is shown in Figure 3. The dopant profile was measured using the electrochemical capacitance-voltage technique.

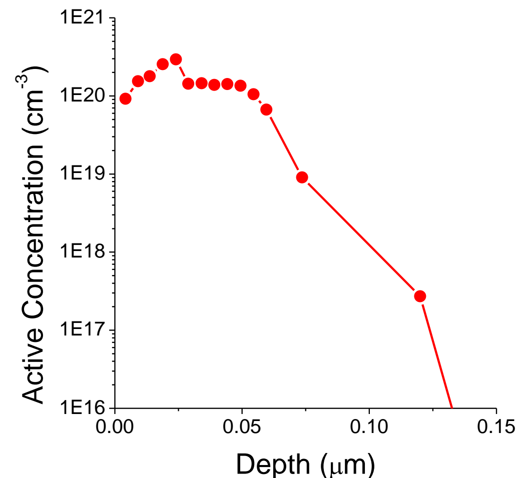

Figure 3: Active dopant concentration for a 40keV, 3×10^{15} cm^{-2} P implant after 10 minutes annealing at 600°C.

The active dopant profile in Figure 3 has high concentration of active dopants near the surface, approaching 1×10^{20} cm^{-3}, and a very shallow depth of doping. The heavily doped, shallow profile is achieved because the low thermal budget of the SPER anneal does not permit significant dopant diffusion. Consequently, the active dopant profile after SPER would be expected to closely approximate the as-implanted profile. This means that higher energy implants would have a deeper doping profile but lower peak concentration for the same dose implanted at lower energy after SPER.

3.2 Contact Resistance

Contact resistivity was measured via the TLM method using thermally evaporated aluminium contact pads. Figure 4 shows the measured contact resistivity as a function of implant energy.

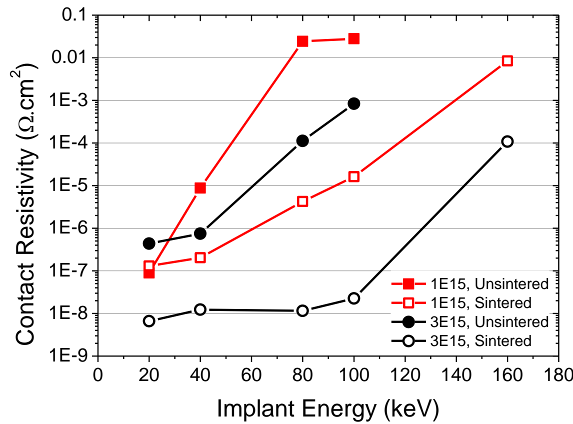

Figure 4: Contact resistivity measured for evaporated aluminium contacts by TLM before and after 250°C, 30 minute sinter.

Contact resistivity below 1×10^{-6} $\Omega.cm^2$ was achieved on the as-evaporated, unsintered contacts for each implant dose at 20 keV, with a trend towards higher contact resistivity for higher implant energy. A 30 minute anneal in forming gas at 250°C improved contact resistivity for all data points. Data for unsintered implants at 160 keV were not included in Figure 4 because ohmic contact was made. Also, for implants at 80keV and 100keV, the implant dose has a more significant impact than at 20 keV and 40keV, with contact resistivity improving with increasing dose. This is expected to be caused by a lower surface concentration for the deeper, more spread out doping profiles resulting from 80 keV or 100 keV implants compared with the shallower implants at 20 keV or 40 keV.

3.3 Recombination Activity

J_{0n+} was measured for unpassivated samples implanted with dose ranging from 1×10^{15} cm^{-2} to 3×10^{15} cm^{-2} and energy from 20keV to 160keV. It is assumed that the surface recombination velocity of the unpassivated surface is sufficiently high to approximate the SRV of a metallised surface, thus replicating surface recombination for contacted regions. The contours of Figure 5 present J_{0n+} in units of $fA.cm^{-2}$ as a function of implant energy and dose. In this figure it is observed that the lowest values of J_{0n+} were measured for samples with the lowest implant energy.

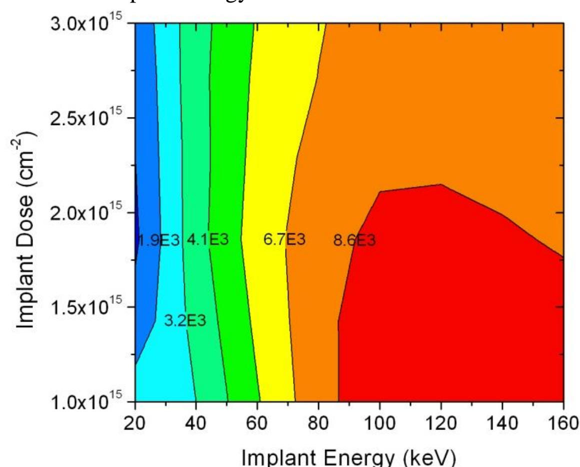

Figure 5: Measured J_{0n+} as a function of implant energy and dose. Values on the contour lines are in $fA.cm^{-2}$.

Also observed in Figure 5 is that for a given implant energy, there is no meaningful variation in J_{0n+} as a function of implant dose, and consequently, sheet resistance.

The relationship between sheet resistance and J_{0n+} is further examined in Figure 6, where samples formed by SPER are directly compared with furnace annealed samples. In this example both furnace and SPER samples were implanted at 40keV, except the SPER samples were cooled during implant to 77K using liquid nitrogen. The furnace annealed samples were subject to 900°C for 30 minutes in O_2 followed by 30 minutes in N_2. Again, the samples were unpassivated to approximate a metallised surface.

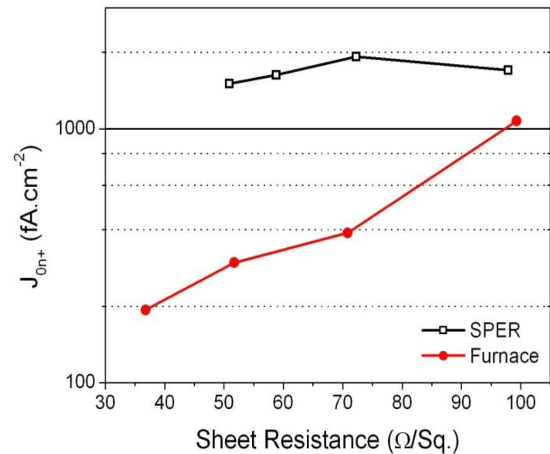

Figure 6: J_{0n+} versus sheet resistance for unpassivated samples prepared with SPER and furnace anneal at 900°C for 60 minutes.

For the furnace anneals, there is a trend towards lower J_{0n+} for lower sheet resistance. This result is expected for a surface with high recombination velocity, as the heavily doped surface regions restrict surface recombination. However, for the SPER samples the correlation between J_{0n+} and sheet resistance is less significant.

If the sample were dominated by recombination at the unpassivated surface, it might be expected that decreasing sheet resistance would reduce J_{0n+}. Conversely, a trend towards higher J_{0n+} with decreasing sheet resistance might indicate the sample is limited by Auger recombination. However, the absence of a strong relationship with sheet resistance suggests that the SPER samples are dominated by neither Auger recombination nor surface recombination.

One possible explanation for the high J_{0n+} is increased S-R-H recombination at the end of the implant range. It is known that SPER does not repair damage in regions that were not amorphised during implantation [3]. In these areas, the primary vacancy and interstitial defects or secondary defects developed during annealing remain are likely to be centres of high S-R-H recombination.

This explanation is supported by comparing samples implanted at 40keV at room temperature (RT) and cooled to 77K with liquid nitrogen (LN) in Figure 7. In each case, the implant dose varied from 1×10^{15} cm^{-2} to 3×10^{15} cm^{-2}.

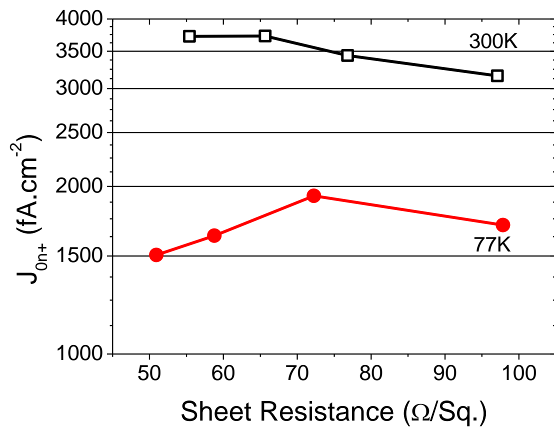

Figure 7: J_{0n+} measured for room temperature (RT) and liquid nitrogen temperature implants (LN).

The effect of implanting at cryogenic temperature is that the amount of primary implant damage is enhanced so that the target wafer is more readily amorphised compared with a room temperature implant [8]. The reason for this is the absence of damage annealing during the implant process. This results in a thicker amorphous layer and a smaller 'damaged crystalline' region at the tail of the implant for the same implant conditions. For samples annealed using SPER, the narrower 'damaged crystalline' region would be expected to contributes less to recombination. In effect, creating more primary damage during implantation increases the effectiveness of SPER, resulting in lower J_{0n+}.

4 CONCLUSIONS

Solid phase epitaxial regrowth has been shown to effectively activate ion implanted phosphorus with a low thermal budget annealing regime. The high concentration of active phosphorus at the surface allows excellent electrical contact to be made to heavily n-type doped regions, although at the expense of high J_{0n+}. The best results for both J_{0n+} and contact resistance were measured for the lowest implant energy, 20keV.

A relationship between decreasing implant energy and decreasing J_{0n+} was observed, while variation in implant dose had a less significant effect on recombination. This can be explained by high S-R-H recombination due to incomplete damage annealing in regions not amorphised by the implant. The high J_{0n+} for SPER samples limits the suitability of this technique for broad area emitter formation, however the low contact resistance achieved means SPER may be suitable for localized, heavily doped regions under electrical contacts.

4.1 Acknowledgements

This Program has been supported by the Australian Government through the Australian Renewable Energy Agency (ARENA). Responsibility for the views, information or advice expressed herein is not accepted by the Australian Government.

7 REFERENCES

[1] J. Benick, R. Muller, N. Bateman, and M. Hermle, "Fully Implanted N-Type PERT Solar Cells," in *27th European PV Solar Energy Conference and Exhibition*, Frankfurt, Germany, 2012.

[2] V. Yelundur, B. Damiani, V. Chandrasekaran, A. Adedokun, A. Payne, X. Wang, *et al.*, "First Implementation of Ion Implantation to Produce Commercial Silicon Solar Cells," *26th European Photovoltaic Solar Energy Conference,* p. 831, 2011.

[3] K. S. Jones, S. Prussin, and E. R. Weber, "A Systematic Analysis of Defects in Ion-Implanted Silicon," *Applied Physics A,* vol. 45, pp. 1-34, 1988/01/01 1988.

[4] Synopsys, "Sentaurus Process User Guide, Version 2013.03," ed, 2013.

[5] G. Olson and J. Roth, "Solid Phase Epitaxy," in *Handbook of Crystal Growth 3 - Thin Films and Epitaxy*, D. Hurle, Ed., ed: Eleseiver, 1994, pp. 257-312.

[6] F. W. Saris, J. S. Custer, R. J. Schreutelkamp, R. J. Liefting, R. Wijburg, and H. Wallinga, "Avoiding dislocations in ion-implanted silicon," *Microelectronic Engineering,* vol. 19, pp. 357-362, 1992.

[7] A. W. Blakers, A. Wang, A. M. Milne, J. Zhao, and M. A. Green, "22.8% efficient silicon solar cell," *Applied Physics Letters,* vol. 55, pp. 1363-1365, 1989.

[8] J. R. Liefting, J. S. Custer, R. J. Schreutelkamp, and F. W. Saris, "Dislocation formation in silicon implanted at different temperatures," *Materials Science and Engineering: B,* vol. 15, pp. 173-186, 1992.